PAPER

On electrical analysis of Al-rich p-AlGaN films for III-nitride UV light emitters

To cite this article: Aakash Jadhav et al 2022 Semicond. Sci. Technol. 37 015003

View the article online for updates and enhancements.

You may also like

- Electrical properties of relaxed p-GaN/p-AlGaN superlattices and their application in ultraviolet-B light-emitting devices
 Kosuke Sato, Shinji Yasue, Yuya Ogino et al.
- Effects of Temperature on InGaN/GaN LEDs with Different MQW Structures Chul Huh and Seong-Ju Park
- Compositionally graded III-nitride alloys: building blocks for efficient ultraviolet optoelectronics and power electronics Haochen Zhang, Chen Huang, Kang Song et al.



Semicond. Sci. Technol. 37 (2022) 015003 (7pp)

https://doi.org/10.1088/1361-6641/ac3710

On electrical analysis of Al-rich p-AlGaN films for III-nitride UV light emitters

Aakash Jadhav¹, Pegah Bagheri², Andrew Klump², Dolar Khachariya³, Seiji Mita⁴, Pramod Reddy⁴, Shashwat Rathkanthiwar², Ronny Kirste⁴, Ramon Collazo², Zlatko Sitar^{2,4} and Biplab Sarkar^{1,2,*}

E-mail: bsarkar@ece.iitr.ac.in

Received 30 June 2021, revised 25 October 2021 Accepted for publication 5 November 2021 Published 26 November 2021



Abstract

In this work, an alternative scheme to estimate the resistivity and ionization energy of Al-rich p-AlGaN epitaxial films is developed using two large-area ohmic contacts. Accordingly, the resistivities measured using current–voltage measurements were observed to corroborate the Hall measurements in the Van der Pauw configuration. A free hole concentration of $\sim\!1.5\times10^{17}~\rm cm^{-3}$ and low ionization energy of $\sim\!65~\rm meV$ in Mg-doped Al $_{0.7}$ Ga $_{0.3}$ N films is demonstrated. Nearly an order of magnitude lower hydrogen concentration than Mg in the as-grown AlGaN films is thought to reduce the Mg passivation and enable higher hole concentrations in Al-rich p-AlGaN films, compared to p-GaN films. The alternate methodology proposed in this work is expected to provide a simpler pathway to evaluate the electrical characteristics of Al-rich p-AlGaN films for future III-nitride ultraviolet light emitters.

Keywords: III-nitride, Mg-doped AlGaN, ionization energy, mobility, contact resistance

1

(Some figures may appear in color only in the online journal)

1. Introduction

Al-rich AlGaN has demonstrated applicability for ultraviolet (UV) light emitters used in applications like water sterilization, UV curing, biomedical instrumentation, etc [1, 2]. These emitters require technologically relevant n-type and ptype resistivities in Al-rich AlGaN films for efficient injection of electrons and holes into the quantum well(s), where they recombine. While a low resistivity of <1 Ω cm in Alrich n-AlGaN (>60% Al mole fraction) films has been widely reported [3–5], achieving a desirable resistivity of <10 Ω cm in Al-rich p-AlGaN films is still a major challenge [6–8]. High resistivity in p-AlGaN has been primarily attributed to

the high acceptor ionization energy (E_A) of Mg, low solubility of Mg leading to its incorporation in electrically inactive sites and relatively low formation energy of compensating defects such as nitrogen-vacancies and Mg-nitrogen vacancy complexes [9]. The value of E_A is believed to increase linearly with Al mole fraction from \sim 120–200 meV (x = 0) [10–12] to \sim 510 meV (x = 1) [6] in p-Al_xGa_{1-x}N. The resulting low free hole concentration at room temperature (RT) leads also to a poor ohmic contact formation and a significant power loss during the device operation [13]. To overcome this difficulty imposed by high E_A in p-AlGaN films, a thin p-GaN layer is typically used for p-side ohmic contact formation in III-nitride UV light emitters [14, 15]. This technique not only introduces processing complexity but also promotes reabsorption of emitted light (in the p-GaN layer due to a lower bandgap), thereby reducing the external quantum efficiency

¹ Department of Electronics and Communication Engineering, Indian Institute of Technology, Roorkee, Uttarakhand 247667, India

² Department of Materials Science and Engineering, North Carolina State University, Raleigh, NC 27606, United States of America

³ Department of Electrical and Computer Engineering, North Carolina State University, Raleigh, NC 27606, United States of America

⁴ Adroit Materials, 2054 Kildaire Farm Road, Suite 205, Cary, NC 27518, United States of America

^{*} Author to whom any correspondence should be addressed.

[16]. Thus, a direct ohmic contact formation to the Al-rich p-AlGaN epitaxial films is necessary to achieve highly efficient UV light emitters. This necessitates the realization of Al-rich p-AlGaN with a low E_A that would result in a high free carrier concentration [13].

Interestingly, a resistivity of 47 Ω cm and a low ionization energy of <100 meV was reported by Kinoshita et al [17] for p-Al_{0.7}Ga_{0.3}N by heavy doping with Mg (\sim 6 × 10¹⁹ cm⁻³). The lower ionization energy was tentatively attributed to an alternate conduction mechanism such as hopping conduction and shows a pathway to achieve higher conductivity in p-AlGaN at higher Mg doping concentrations as long as the compensation is reduced. Two modified approaches have been recently developed to achieve a higher free carrier concentration in Al-rich p-AlGaN films. These include the distributed polarization doping technique, which uses a linearly, compositionally graded Mg-doped AlGaN layer [18-20], and the short period superlattice technique, which uses superlattice structures consisting of alternate p-Al_xGa_{1-x}N/p-Al_yGa_{1-y}N $(0 \le x \le 1, 0 \le y \le 1, x \ne y)$ layers [21, 22]. These techniques demand precise control over thickness and composition in the AlGaN epitaxial films. A few reports have highlighted the possibility of achieving a low E_A in Mg-doped bulk Al-rich p-AlGaN films [17, 23]. However, poor hole mobility, due to alloy scattering in Al-rich p-AlGaN [24], along with poor ohmic contacts restricted the determination of $E_{\rm A}$ using the traditional DC Hall measurement due to low Hall voltages.

In this work, we report on the observation of low acceptor ionization energy of \sim 65 meV in Mg-doped p-Al $_{0.7}$ Ga $_{0.3}$ N epitaxial films measured using AC Hall measurements. A simpler methodology (using two large area Ni/Au contacts) to estimate the $E_{\rm A}$ in Al-rich p-AlGaN films using temperature-dependent current-voltage (I-V) measurements is shown to corroborate the Hall measurements. The benefit of a significantly larger change in the temperature dependence of free hole concentration as compared to the hole mobility is shown to be effective in determining the $E_{\rm A}$ using I-V measurements.

2. Materials and methods

Mg-doped p-Al_{0.7}Ga_{0.3}N films were grown on sapphire substrates using low-pressure metalorganic vapor phase epitaxy (LP-MOVPE) [25, 26]. The reactor pressure was kept constant at 20 Torr throughout the growth. The growth consisted of a 400 nm thick AlN layer, followed by a 600 nm Mg-doped p-Al_{0.7}Ga_{0.3}N layer. Trimethylaluminum, triethylgallium, and ammonia gas were used as the Al, Ga, and N precursors, respectively. The film was doped with Mg using Bis-cyclopentadienyl-magnesium (Cp₂Mg) to a doping level of $\sim 2 \times 10^{19}$ cm⁻³. The p-Al_{0.7}Ga_{0.3}N films were grown at a temperature of 1100 °C in H₂ diluent/carrier gas with a total reactor flow rate of 11 slm. The V/III ratio was kept at 2000 to minimize the incorporation of V_N^{3+} self-compensating defects in p-Al_{0.7}Ga_{0.3}N [17]. After the growth, the Mg dopant activation anneal was performed either in air or N₂ ambient. Few

samples were not annealed, whereas the dopant activation temperature used for other samples used in this work will be discussed later. All the activation anneals were carried out for 20 min. Anneals under air ambient were carried out inside a tube furnace, whereas anneals under N_2 ambient were carried out inside the LP-MOVPE chamber.

For the large area ohmic contact formation, the activated p-Al_{0.7}Ga_{0.3}N wafer was cleaned using acetone, methanol, and DI water, followed by dipping in 1% HF and hot 1:1 HCl:H₂O solutions [13]. Conventional photolithography was used to pattern the contacts on p-Al_{0.7}Ga_{0.3}N layers, followed by the metal deposition and lift-off. Standard Ni (20 nm)/Au (40 nm) contacts were deposited using ultra-high vacuum ebeam evaporation (base pressure: 1×10^{-9} Torr). The contacts were annealed at 600 °C for 10 min in air ambient. The contact geometry consisted of an infinite area contact, a known diameter large-area contact, and a known separation between the contacts. In this work, the diameter of the large area contact and the separation between the contacts were chosen to be $600 \mu m$ and $100 \mu m$, respectively. For AC Hall measurements, Ni/Au contacts were deposited and annealed on a squareshaped sample using the Van der Pauw geometry. AC Hall measurements were performed in an 8400 series LakeShore AC/DC Hall measurement system using a magnetic field and excitation field frequency of ~ 0.62 T and 100 mHz, respectively.

For comparing the $E_{\rm A}$ in p-Al_{0.7}Ga_{0.3}N with p-GaN, a p-GaN reference sample having a similar Mg doping concentration ($\sim 2 \times 10^{19}$ cm⁻³) was also grown on a sapphire substrate. Further details about the p-GaN growth and surface cleaning procedures can be found elsewhere [10]. Standard Ni/Au contacts with geometry similar to the p-Al_{0.7}Ga_{0.3}N were formed on p-GaN for I-V (large area contacts) and Hall measurements (Van der Pauw geometry). Temperature-dependent I-V measurements were performed using Keithley 4200 semiconductor parameter analyzer. Calculations and curve fittings were carried out using MATLAB software. Doping levels, oxygen and carbon impurity concentrations were measured using secondary ion mass spectroscopy (SIMS) performed by EAG.

3. Results and discussion

The variation of free hole concentration and hole mobility in p-Al_{0.7}Ga_{0.3}N and the p-GaN reference sample were measured using Hall measurements, as shown in figure 1(a). A RT free hole concentration of $\sim 1.5 \times 10^{17}$ cm⁻³ is obtained in p-Al_{0.7}Ga_{0.3}N, which increases to $4-5 \times 10^{17}$ cm⁻³ at temperatures of actual light emitter operation (~ 100 °C) [10]. The variation of free hole concentration with temperature (T) in p-GaN is observed to show a larger slope compared to the p-Al_{0.7}Ga_{0.3}N. The free hole concentration (p) was fitted using the following equation to extract E_A [10]:

$$\frac{p(p+N_{\rm D})}{N_{\rm A}-N_{\rm D}-p} = \frac{N_{\rm V}}{g} \exp\left(-\frac{E_{\rm A}}{kT}\right),\tag{1}$$

where $N_{\rm D}$ is the compensating donor concentration, $N_{\rm A}$ is the Mg doping concentration, $N_{\rm V}$ is the effective density of

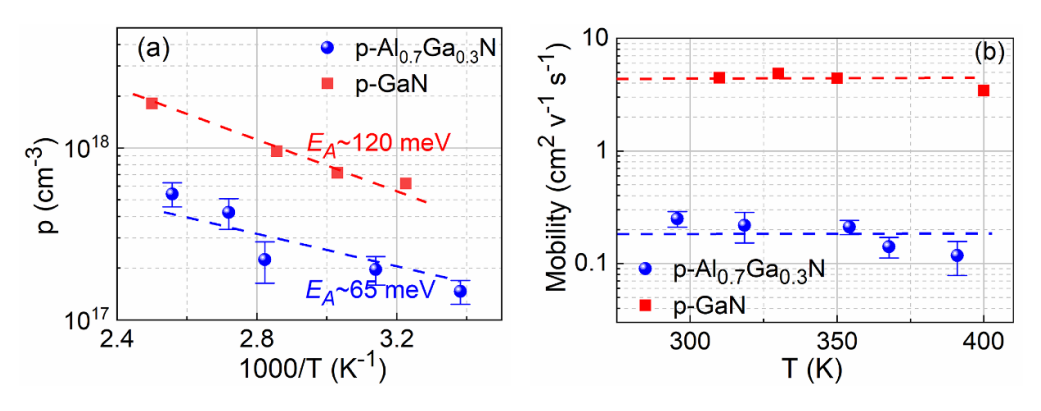


Figure 1. The variation of (a) free hole concentration and (b) mobility in p-GaN and p-Al_{0.7}Ga_{0.3}N layers as observed using Hall measurements.

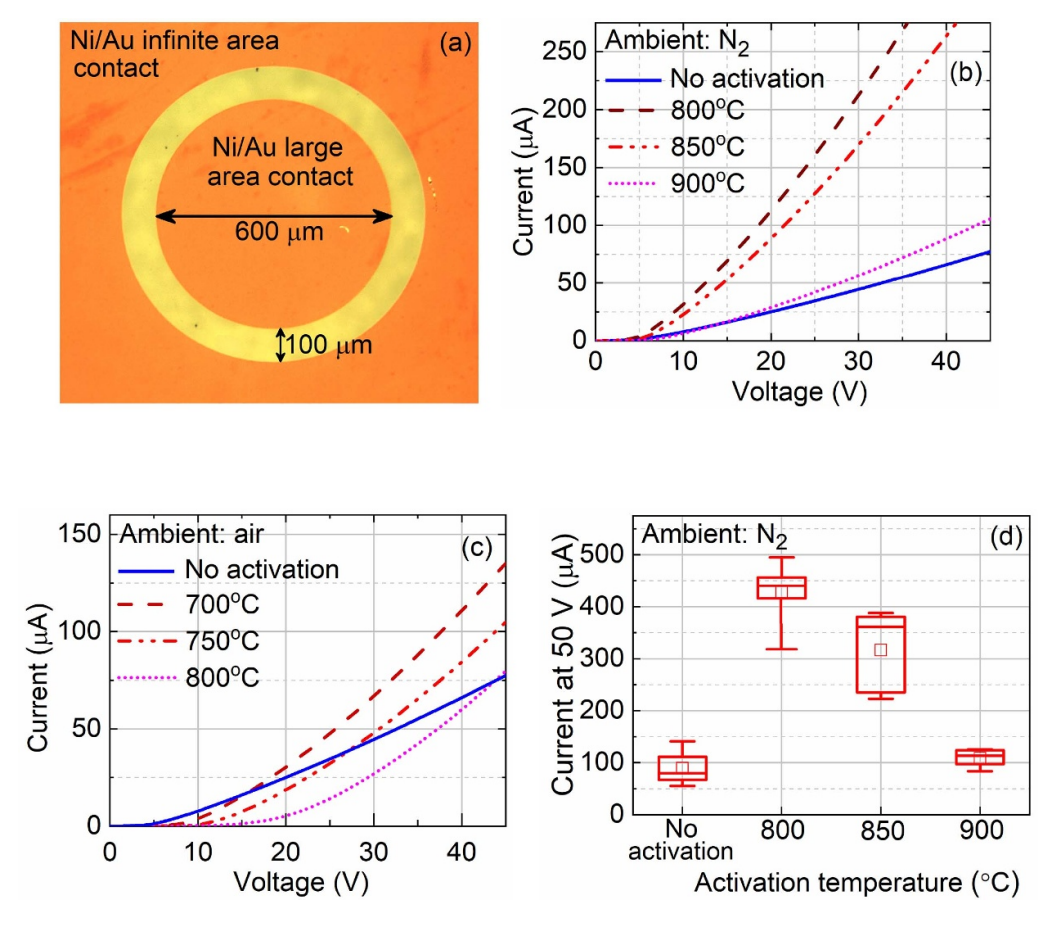
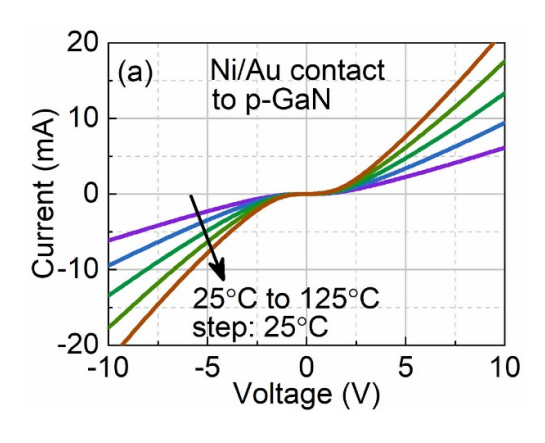


Figure 2. (a) Contact geometry used to determine E_A in p-Al_{0.7}Ga_{0.3}N; (b), (c) I-V characteristics of Ni/Au contacts to p-Al_{0.7}Ga_{0.3}N for different activation anneal schemes, and (d) current at 50 V through contacts fabricated across the wafers either non-activated or activated under N₂ ambient.

states in the valence band, g is the acceptor degeneracy factor (g=4 for holes) and k is the Boltzmann constant. The ionization energy for Mg in p-GaN reference wafer was observed to be $\sim 120 \pm 5$ meV, closely resembling the previously reported values for p-GaN [11, 12]. In contrast, Mg doping in p-Al_{0.7}Ga_{0.3}N showed an $E_{\rm A}$ of $\sim 65 \pm 8$ meV for a similar temperature range. The corresponding values of $N_{\rm D}$ derived using the least-square error technique were observed to be $\sim 1.5 \times 10^{19}$ cm⁻³ and $\sim 5 \times 10^{18}$ cm⁻³ in p-AlGaN and p-GaN, respectively. The mobility follows a rather shallow trend

with temperature change, as observed in figure 1(b). From RT to \sim 85 °C, the mobility is observed to be nearly constant, while the hole concentration changes significantly. Therefore, the variation in resistivity with temperature is primarily caused by the change in free hole concentration in the epitaxial films. This indicates that the variation in sheet resistivity observed in I-V measurements can also be used to estimate the acceptor $E_{\rm A}$. To verify this hypothesis, the resistivity was recorded using I-V measurements using the contact geometry shown in figure 2(a). Two large area ohmic contacts were fabricated



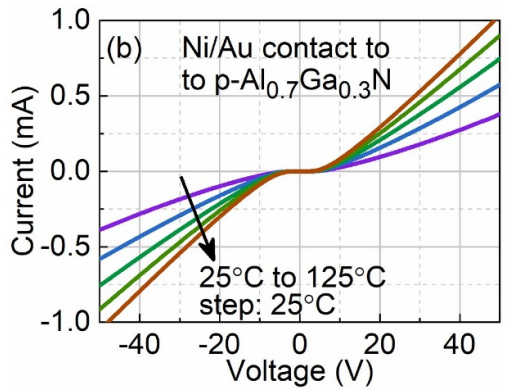


Figure 3. I-V characteristics of Ni/Au contact to (a) p-GaN and (b) p-Al_{0.7}Ga_{0.3}N having the contact geometry shown in figure 2(a).

on the p-GaN and p- $Al_{0.7}Ga_{0.3}N$ to ensure low contact resistance.

Figures 2(b) and (c) shows the *I–V* characteristics of standard Ni/Au ohmic contacts to p-Al_{0.7}Ga_{0.3}N for different activation schemes. Unlike p-GaN, p-Al_{0.7}Ga_{0.3}N films showed reasonable current flow through the Ni/Au contacts even without activation anneal, as observed in figure 2(b). An increase in the current was observed after an activation anneal at 800 °C under N₂ ambient. Further increase in the activation anneal temperature in N₂ ambient resulted in a lower current through the contacts, likely due to Mg self-compensation or formation of vacancy-related complexes [9]. On the contrary, a conventional activation scheme typically performed for p-GaN (600 °C–700 °C in air ambient) was observed to result in resistive *I–V* characteristics for p-Al_{0.7}Ga_{0.3}N, shown in figure 2(c).

The nonlinear threshold-type I-V characteristics can be attributed to the commonly observed potential barrier at the metal-semiconductor interface [13]. Up to a certain turn-on voltage ($V_{\text{turn-on}}$), the current through the metal-semiconductor interface is restricted by the high contact resistance arising due to the barrier potential. However, once applied voltage exceeds $V_{\text{turn-on}}$, the Ni/Au contact starts conducting and the current is mostly limited by the sheet resistance of the semiconductor. A higher V_{turn-on} observed for air annealed p-Al_{0.7}Ga_{0.3}N may be due to the formation of a thin AlO_x layer after the activation anneal. The observed increase in $V_{\text{turn-on}}$ at higher air anneal temperatures (in air ambient) further reaffirms the possibility of forming AlO_x. The variations in current through the contacts in different areas of the wafer either without activation anneal or activation anneal under N2 ambient are highlighted in figure 2(d). In general, p-Al_{0.7}Ga_{0.3}N film that had an activation anneal at 800 °C under N₂ ambient showed a higher current compared to any other activation anneal schemes. Thus, the activation anneal for p-Al_{0.7}Ga_{0.3}N was fixed at 800 °C for 20 min in N_2 ambient for the remaining analyses.

Temperature-dependent I-V characteristics of Ni/Au ohmic contact to the p-GaN and p-Al_{0.7}Ga_{0.3}N samples having the large area contact geometry are shown in figure 3. Temperature range was limited to \sim 400 K so that mobility remains nearly constant (see figure 1(b)). Significantly

higher hole mobility in p-GaN results in lower sheet resistance and higher current values. However, a higher $V_{\rm turn-on}$ at the metal/p-Al_{0.7}Ga_{0.3}N interface indicates a larger barrier potential. At an applied voltage much larger than the $V_{\rm turn-on}$, the differential resistance ($R_{\rm Diff}$) from the I-V characteristics at different temperatures can be written as:

$$R_{\text{Diff}} = R_{\text{CI}} + R_{\text{CL}} + R_{\text{Semi}}, \tag{2}$$

where $R_{\rm CI}$, $R_{\rm CL}$, and $R_{\rm Semi}$ are the contact resistance of infinite area outer contact, large area inner circular contact, and the semiconductor sheet resistance of p-GaN or p-Al_{0.7}Ga_{0.3}N, respectively. The values of $R_{\rm Diff}$ for the p-GaN and p-AlGaN films were calculated from I-V curves in the range 5–10 V and 40–50 V, respectively. Since the contacts occupy a large area, the ($R_{\rm CI}+R_{\rm CL}$) term of equation (2) can be considered much lower than the $R_{\rm Semi}$. Thus, $R_{\rm Diff}$ can be used to estimate the resistivity of the semiconductor at different temperatures using the relation [27]:

$$\rho_{\rm I-V} = \frac{R_{\rm Diff} t_{\rm epi} F}{C},\tag{3}$$

where $\rho_{\rm I-V}$ is the semiconductor resistivity (in Ω cm) to be calculated from the temperature-dependent I-V characteristics, $t_{\rm epi}$ is the thickness of the semiconductor epitaxial film, F is the area factor, and C is a correction factor given as:

$$F = \frac{2\pi r_{\rm S}}{d} \tag{4}$$

$$C = \frac{r_s}{d} \ln \left(\frac{r_s + d}{r_s} \right) \tag{5}$$

where $r_{\rm S}$ is the radius of the inner circular contact and d is the contact separation. For the geometry used in this work, $r_{\rm S} \approx 330~\mu{\rm m}$, and $d \approx 100~\mu{\rm m}$, the values of C and F were found to be $\sim\!0.9$ and $\sim\!18.7$, respectively. The resistivities of p-GaN and p-Al_{0.7}Ga_{0.3}N as calculated from the I-V characteristics using equation (2) and as measured by Hall are shown in figure 4(a).

The resistivities of p-GaN and p-Al_{0.7}Ga_{0.3}N measured in the Van der Pauw geometry and calculated from the I-V curves

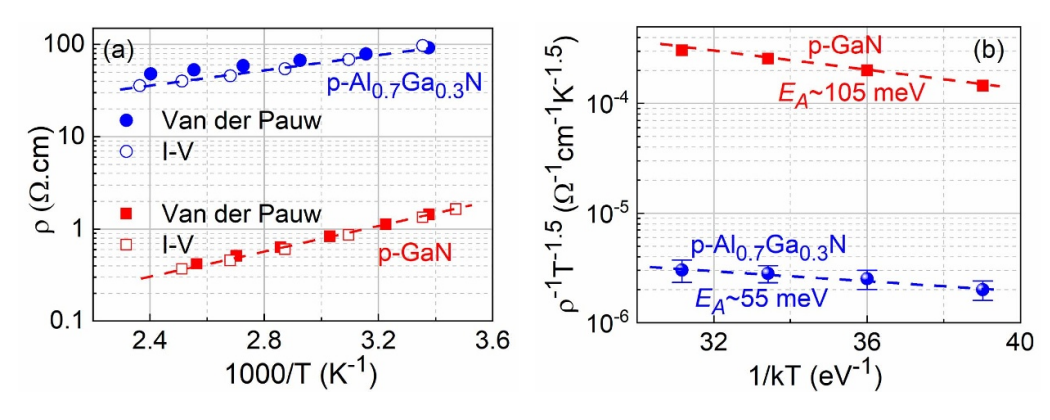


Figure 4. (a) Resistivity (ρ) vs 1000/T plot for p-GaN and p-Al_{0.7}Ga_{0.3}N obtained from Van der Pauw and I-V measurements and (b) $\rho^{-1}T^{-1.5}$ vs 1/kT plot (up to \sim 85 °C) where ρ is taken from the I-V measurements.

agree well, indicating the accuracy of the resistivity extraction methodology using large area contacts. To the 1st-order approximation (considering $N_{\rm A}$ and $N_{\rm D} \gg p$), equation (1) can be rewritten as:

$$p \approx \frac{(N_{\rm A} - N_{\rm D}) N_{\rm V}}{g N_{\rm D}} \exp\left(-\frac{E_{\rm A}}{kT}\right).$$
 (6)

In the above equation, $N_{\rm A}$, $N_{\rm D}$, and g are independent of temperature, whereas $N_{\rm V}$ has a temperature dependence ($N_{\rm V} \propto T^{1.5}$). As observed in figure 1(b), the mobility is nearly constant up to $\sim\!85\,^{\circ}{\rm C}$. Therefore, multiplying both sides of the equation (6) with electronic charge (q) and mobility, an equation relating the resistivity and $E_{\rm A}$ can be written as:

$$\rho^{-1}T^{-1.5} \approx \beta \exp\left(-\frac{E_{\rm A}}{kT}\right),\tag{7}$$

where β is a constant term comprising the multiplication of q, mobility, and all temperature-independent terms of equation (6), and ρ is the resistivity calculated from the I-V measurements. Therefore, the slope of $\ln(\rho^{-1}T^{-1.5})$ vs 1/kT characteristics can be used to extract the E_A if the mobility is constant. Values of E_A derived from the temperature-dependent I-V measurements and equation (7) are ~ 105 meV and ~ 55 meV for p-GaN and p-Al_{0.7}Ga_{0.3}N, respectively. Error margin observed in both these values are within ± 5 meV. Both values are in good agreement with the values obtained using Hall measurements (figure 1(a)). Therefore, I-V measurements using large area contacts offer a simple methodology to complement the E_A in Al-rich p-AlGaN films estimated using Hall measurements.

The low E_A observed in Al-rich p-AlGaN films indicates a significant contribution from hole hopping or impurity band conduction mechanism instead of a pure valence band transport as suggested in [17]. Similar behavior has been observed in p-type GaN and InGaN films, although at relatively low temperatures [28, 29]. The observation of impurity band conduction at RT in this study is possibly related to the low valence band mobility in Al-rich AlGaN, although more investigation is necessary to quantitatively understand the

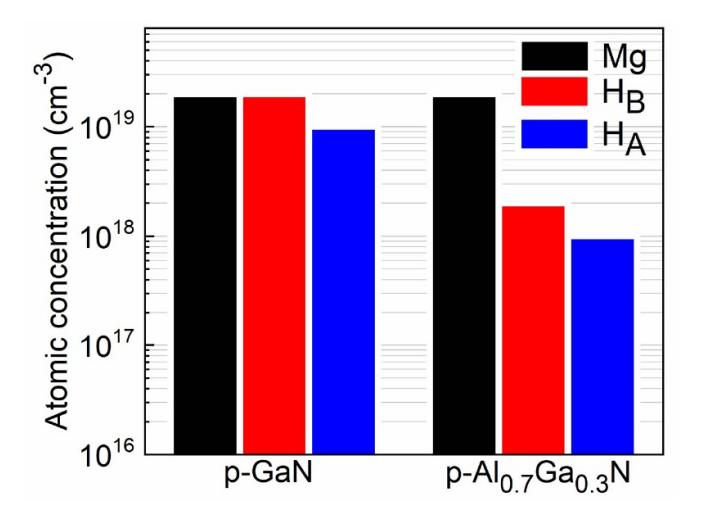


Figure 5. Atomic concentration of Mg and H in p-GaN and p-Al_{0.7}Ga_{0.3}N films; H_B and H_A represents the H concentration before and after dopant activation anneal, respectively.

individual contributions from the valence band and impurity band transport mechanisms. Interestingly, suppressed incorporation of H was observed during the growth of p-AlGaN films. Figure 5 shows the concentration of Mg and H in p-GaN and p-Al_{0.7}Ga_{0.3}N films measured using SIMS. The concentration of H in p-GaN closely follows the Mg doping concentration (figure 5), which is believed to passivate a majority of the Mg-dopants by forming Mg-H complexes [30–33]. On the contrary, H concentration in p-Al_{0.7}Ga_{0.3}N film was observed to be nearly an order of magnitude lower for a similar Mg doping concentration. Therefore, the density of the Mg-H complexes in p-Al_{0.7}Ga_{0.3}N is likely to be much lower than that of p-GaN, indicating a higher concentration of non-passivated Mg dopants in as-grown p-Al_{0.7}Ga_{0.3}N. Accordingly, appreciable conductivity was observed for nonactivated p-Al_{0.7}Ga_{0.3}N films (figures 2(b) and (d)). This contrasts with non-activated p-GaN films that are by and large highly resistive. Further reduction of H concentration in p-Al_{0.7}Ga_{0.3}N is possible by performing an activation anneal

Table 1. Recent reports on p, ρ and E_A of bulk p-AlGaN films at RT.

Composition	$p (\mathrm{cm}^{-3})$	$\rho \atop (\Omega \text{ cm})$	E _A (meV)	Reference
p-Al _{0.7} Ga _{0.3} N p-Al _{0.7} Ga _{0.3} N	$\sim 1.5 \times 10^{17}$ 1.3×10^{17}	~91 47	~65 47–72	This work Kinoshita <i>et al</i> [17]
$\begin{array}{l} p\text{-}Al_{0.6}Ga_{0.4}N \\ p\text{-}Al_{0.4}Ga_{0.6}N \\ p\text{-}Al_{0.4}Ga_{0.6}N \end{array}$	8.7×10^{17} 3.26×10^{17} 4.97×10^{18}	0.7 — 0.93	≤11 46 39 ± 3	Liu et al [9] Chen et al [34] Qiu et al [8]

at 800 °C under N2 ambient, as observed in figure 5. Despite the low ionization energy, a lower free hole concentration was observed in p-Al_{0.7}Ga_{0.3}N compared to p-GaN. This is attributed to a higher density of (non-hydrogen) donor-type compensating point defects present in the p-Al_{0.7}Ga_{0.3}N films such as nitrogen-vacancies and Mg nitrogen-vacancy complexes. Indeed, a high $N_{\rm D}$ of 1.5 \times 10¹⁹ cm⁻³ was estimated from charge balance fittings to the temperature-dependent Hall measurements in figure 1(a). Firstly, this is related to relatively low formation energies of these defects in Al-rich AlGaN as compared to GaN. Secondly, the high density of non-passivated Mg atoms would shift the quasi-Fermi level closer to the valence band during the growth, further reducing the formation energy of these defects. Furthermore, a high current observed in non-activated films (figures 2(b) and (d)) also indicate that a large number of Mg dopants successfully substituted the group-III elements in p-Al_{0.7}Ga_{0.3}N during growth. A comparison of the values of free hole concentration (p), resistivity (ρ) and E_A obtained in this work with other literature reports for bulk Mg-doped AlGaN films are highlighted in table 1.

At this point, it is necessary to highlight the importance of the I-V measurement methodology developed to estimate the E_A in Al-rich p-AlGaN films. The low hole mobility, likely due to significant alloy scattering or contributions from hopping transport in p-AlGaN [17] results in relatively low Hall coefficients. This poses limitations in the accurate determination of free hole concentration and E_A using the commonly used DC Hall measurements. The AC Hall measurements employed in this work can reliably measure much lower Hall coefficients by effectively reducing the error components involved. It has to be noted that the resistivity extraction methodology may result in an overestimation of E_A if the mobility variation with temperature is large compared to the change in carrier concentration, as seen in figure 1. Furthermore, the estimation of E_A highlighted in this work may not be valid for a wider temperature range, as different ionization or conduction mechanisms dominate at different temperatures in p-AlGaN [9].

Furthermore, both the n-type and p-type contacts to III-nitrides are alloyed contacts where the contact resistance is a strong function of the free carrier concentration in the epitaxial film [13, 35], Hall measurements are trustable only when the contacts used for the measurement possess acceptable resistivity values. The coincidence in value of E_A estimated using Hall measurements and I-V measurements ensures

that Hall measurements performed on Al-rich p-AlGaN films are trustable, and vice-versa. Thus, the alternate technique (using large area Ni/Au contacts) used in this work corroborates the resistivity and E_A estimated using Hall measurements. It is important to note that low mobility is detrimental for lateral devices where the current flow experiences a high semiconductor sheet resistance in high-frequency switching devices. On the other hand, the presence of a high free hole concentration coupled with sufficient electric field can assist significant hole injection into the active region of vertical and/or quasi-vertical optoelectronic devices. Finally, while Si-doping in Al-rich AlGaN is already known to offer $E_A < 50$ meV [4], a low value of E_A in Al-rich p-AlGaN films reported is considered to be instrumental in assisting the development of III-nitride UV light emitters.

4. Conclusions

In this work, a low ionization energy (\sim 65 meV) is demonstrated in p-Al_{0.7}Ga_{0.3}N bulk epitaxial films grown using LP-MOVPE. Unlike p-GaN, nearly an order of magnitude lower hydrogen concentration compared to the magnesium doping concentration is observed in p-Al_{0.7}Ga_{0.3}N epitaxial films. Furthermore, current–voltage measurements using large area Ni/Au contacts were shown to corroborate the low ionization energy observed in Al-rich p-AlGaN epitaxial films. Technologically relevant free hole concentration of \sim 1.5 \times 10¹⁷ cm⁻³ observed in p-Al_{0.7}Ga_{0.3}N films in this study is promising toward the development of future III-nitride UV light emitters.

Data availability statement

All data that support the findings of this study are included within the article.

Acknowledgments

The authors acknowledge funding in part from Air Force Office of Scientific Research (FA9550-17-1-0225, FA9550-19-1-0114), National Science Foundation (ECCS-1916800, ECCS-1653383), and Army Research Office (W911NF-20-C-0020).

ORCID iDs

Pegah Bagheri https://orcid.org/0000-0002-1880-4811
Dolar Khachariya https://orcid.org/0000-0002-8780-4583
Pramod Reddy https://orcid.org/0000-0002-8556-1178
Shashwat Rathkanthiwar https://orcid.org/0000-0003-0180-1398
Zlatko Sitar https://orcid.org/0000-0002-7385-0837

Biplab Sarkar https://orcid.org/0000-0003-0074-0626

References

- [1] Tsao J Y *et al* 2018 Ultrawide-bandgap semiconductors: research opportunities and challenges *Adv. Electron. Mater.* **4** 1600501
- [2] Amano H et al 2020 The 2020 UV emitter roadmap J. Phys. Appl. Phys. 53 503001
- [3] Mehnke F, Wernicke T, Pingel H, Kuhn C, Reich C, Kueller V, Knauer A, Lapeyrade M, Weyers M and Kneissl M 2013 Highly conductive n-Al_xGa_{1-x}N layers with aluminum mole fractions above 80% Appl. Phys. Lett. 103 212109
- [4] Bryan I et al 2018 Doping and compensation in Al-rich AlGaN grown on single crystal AlN and sapphire by MOCVD Appl. Phys. Lett. 112 062102
- [5] Washiyama S et al 2020 The role of chemical potential in compensation control in Si:AlGaN J. Appl. Phys.
 127 105702
- [6] Zheng T C, Lin W, Liu R, Cai D J, Li J C, Li S P and Kang J Y 2016 Improved p-type conductivity in Al-rich AlGaN using multidimensional Mg-doped superlattices Sci. Rep. 6 21897
- [7] Dalmau R and Moody B 2018 (Invited) polarization-induced doping in graded AlGaN epilayers grown on AlN single crystal substrates ECS Trans. 86 31
- [8] Qiu X, Chen Y, Han E, Lv Z, Song Z and Jiang H 2020 High doping efficiency in p-type Al-rich AlGaN by modifying the Mg doping planes Mater. Adv. 1 77–85
- [9] Liu X, Pandey A, Laleyan D A, Mashooq K, Reid E T, Shin W J and Mi Z 2018 Charge carrier transport properties of Mg-doped Al_{0.6}Ga_{0.4}N grown by molecular beam epitaxy Semicond. Sci. Technol. 33 085005
- [10] Sarkar B et al 2017 High free carrier concentration in p-GaN grown on AlN substrates Appl. Phys. Lett. 111 032109
- [11] Chen Y, Wu H, Yue G, Chen Z, Zheng Z, Wu Z, Wang G and Jiang H 2015 Analysis on the enhanced hole concentration in p-type GaN grown by indium-surfactant-assisted Mg delta doping *Phys. Status Solidi* b **252** 1109–15
- [12] Reshchikov M A, Ghimire P and Demchenko D O 2018 Magnesium acceptor in gallium nitride. I. Photoluminescence from Mg-doped GaN *Phys. Rev.* B 97 205204
- [13] Sarkar B, Reddy P, Klump A, Kaess F, Rounds R, Kirste R, Mita S, Kohn E, Collazo R and Sitar Z 2018 On Ni/Au alloyed contacts to Mg-doped GaN J. Electron. Mater. 47 305–11
- [14] Park J-S, Kim J K, Cho J and Seong T-Y 2017 Review—group III-nitride-based ultraviolet light-emitting diodes: ways of increasing external quantum efficiency *ECS J. Solid State Sci. Technol.* 6 Q42–52
- [15] Zhang Z, Kushimoto M, Sakai T, Sugiyama N, Schowalter L J, Sasaoka C and Amano H 2019 A 271.8 nm deep-ultraviolet laser diode for room temperature operation *Appl. Phys. Express* 12 124003
- [16] Ryu H-Y, Choi I-G, Choi H-S and Shim J-I 2013 Investigation of light extraction efficiency in AlGaN deep-ultraviolet light-emitting diodes Appl. Phys. Express 6 062101
- [17] Kinoshita T, Obata T, Yanagi H and Inoue S 2013 High p-type conduction in high-Al content Mg-doped AlGaN Appl. Phys. Lett. 102 012105
- [18] Simon J, Protasenko V, Lian C, Xing H and Jena D 2010 Polarization-induced hole doping in wide–band-gap

- uniaxial semiconductor heterostructures *Science* **327** 60–64
- [19] Sun L, Lv Z, Zhang Z, Qiu X and Jiang H 2020 High-performance AlGaN heterojunction phototransistor with dopant-free polarization-doped P-base *IEEE Electron Device Lett.* 41 325–8
- [20] Omori T et al 2020 Internal loss of AlGaN-based ultraviolet-B band laser diodes with p-type AlGaN cladding layer using polarization doping Appl. Phys. Express 13 071008
- [21] Martens M et al 2016 Low absorption loss p-AlGaN superlattice cladding layer for current-injection deep ultraviolet laser diodes Appl. Phys. Lett. 108 151108
- [22] Duboz J-Y 2014 GaN/AlGaN superlattices for p contacts in LEDs Semicond. Sci. Technol. 29 035017
- [23] Aoyagi Y, Takeuchi M, Iwai S and Hirayama H 2012 Formation of AlGaN and GaN epitaxial layer with high p-carrier concentration by pulse supply of source gases AIP Adv. 2 012177
- [24] Nakarmi M L, Kim K H, Khizar M, Fan Z Y, Lin J Y and Jiang H X 2005 Electrical and optical properties of Mg-doped Al_{0.7}Ga_{0.3}N alloys Appl. Phys. Lett. 86 092108
- [25] Bryan Z *et al* 2013 Fermi level control of point defects during growth of Mg-doped GaN *J. Electron. Mater.* 42 815–9
- [26] Kirste R et al 2013 Compensation effects in GaN:Mg probed by Raman spectroscopy and photoluminescence measurements J. Appl. Phys. 113 103504
- [27] Klootwijk J H and Timmering C E 2004 Merits and limitations of circular TLM structures for contact resistance determination for novel III–V HBTs Proc. 2004 Int. Conf. on Microelectronic Test Structures (IEEE Cat. No. 04CH37516) pp 247–52
- [28] Kumakura K, Makimoto T and Kobayashi N 2003 Mg-acceptor activation mechanism and transport characteristics in p-type InGaN grown by metalorganic vapor phase epitaxy J. Appl. Phys. 93 3370–5
- [29] Gunning B, Lowder J, Moseley M and Alan Doolittle W 2012 Negligible carrier freeze-out facilitated by impurity band conduction in highly p-type GaN Appl. Phys. Lett. 101 082106
- [30] Nakamura S, Iwasa N, Senoh M and Mukai T 1992 Hole compensation mechanism of P-type GaN films *Jpn. J. Appl. Phys.* 31 1258–66
- [31] Klump A, Hoffmann M P, Kaess F, Tweedie J, Reddy P, Kirste R, Sitar Z and Collazo R 2020 Control of passivation and compensation in Mg-doped GaN by defect quasi Fermi level control J. Appl. Phys. 127 045702
- [32] Nakagawa Y et al 2004 Hydrogen dissociation from Mg-doped GaN Jpn. J. Appl. Phys. 43 23
- [33] Lee J K, Hyeon G Y, Tawfik W Z, Choi H S, Ryu S-W, Jeong T, Jung E and Kim H 2015 Electrochemical removal of hydrogen atoms in Mg-doped GaN epitaxial layers J. Appl. Phys. 117 185702
- [34] Chen Y, Wu H, Han E, Yue G, Chen Z, Wu Z, Wang G and Jiang H 2015 High hole concentration in p-type AlGaN by indium-surfactant-assisted Mg-delta doping *Appl. Phys. Lett.* **106** 162102
- [35] Mohammad S N 2004 Contact mechanisms and design principles for alloyed ohmic contacts to n-GaN J. Appl. Phys. 95 7940–53